Performance Evaluation of Impulse Radio UWB Systems with Pulse-Based Polarity Randomization in Asynchronous Multiuser Environments[1]

Sinan Gezici, Hisashi Kobayashi and H. Vincent Poor[1]
Department of Electrical Engineering
Princeton University, Princeton, NJ 08544
{sgezici,hisashi,poor}@princeton.edu

Andreas F. Molisch[2]
Mitsubishi Electric Research Laboratories
201 Broadway, Cambridge, MA 02139
Andreas.Molisch@ieee.org

***Abstract*— The performance of a binary phase shift keyed random time-hopping impulse radio system with pulse-based polarity randomization is analyzed. The effects of multiple access interference are investigated for both chip-synchronous and asynchronous systems. It is shown that the performance of a chip-synchronous system is the same as that for the symbol-synchronous case studied in [7]. The asynchronous system is modelled as a chip-synchronous system with uniformly distributed timing jitter on the transmitted pulses of interfering users. This extends the analytical technique developed for the chip-synchronous case to the asynchronous case. An approximate closed-form expression for the probability of error, expressed in terms of the autocorrelation function of the transmitted pulse, is derived for the asynchronous case. The analysis shows that the chip-synchronous assumption can result in over-estimating the error probability, and hence that the system design based on this approximation will be on the safe side. The degree of over-estimation mainly depends on the autocorrelation function of the UWB pulse and signal-to-interference-plus-noise-ratio (SIR) of the system. Simulations studies support this approximate analysis.**

***Keywords*— Ultra-wideband (UWB), impulse radio (IR), multiple access interference (MAI), asynchronous systems.**

I. Introduction

Since the US Federal Communications Commission (FCC) approved the limited use of ultra-wideband (UWB) technology [2], communications systems that employ UWB signals have drawn considerable attention. A UWB signal is defined as one that possesses a bandwidth larger than 500MHz and can coexist with with incumbent systems in the same frequency range due to its large spreading factor and low power spectral density. UWB technology holds great promise for a variety of applications such as short-range high-speed data transmission and precise location estimation.

Commonly, impulse radio (IR) systems, which transmit very short pulses with a low duty cycle, are employed to implement UWB systems ([3]-[5]). In an IR system, a train of pulses is sent and information is usually conveyed by the positions or the polarities of the pulses, which correspond respectively to Pulse Position Modulation (PPM) and Binary Phase Shift Keying (BPSK)[3], respectively. In order to prevent catastrophic collisions among different users and thus provide robustness against multiple access interference, each information symbol is represented by a sequence of pulses; the positions of the pulses within that sequence are determined by a pseudo-random time-hopping (TH) sequence specific to each user [3]. The number N_f of pulses representing one information symbol can also be interpreted as a pulse combining gain. An additional "pulse spreading gain" N_c is equal to the ratio of the average time between pulses, and the pulse width.

In "classical" impulse radio, the polarities of those N_f pulses representing an information symbol are always the same, no matter whether PPM or BPSK is employed ([3], [6]). Recently, pulse-based polarity randomization was proposed, where each pulse has a random polarity code (± 1) in addition to the modulation scheme ([7], [8]). The use of polarity codes can provide additional robustness against multiple access interference and help to optimize the spectral shape according to FCC specifications by eliminating the spectral lines inherent in IR systems not using polarity randomization [10].

In this paper, we study the performance of a TH-IR system with pulse-based polarity randomization and provide (approximate) closed-form expressions. We consider the practically important case in which different users are completely unsynchronized. We start out by considering the chip-synchronous case, in which the symbols of different users are misaligned but this misalignment is an integer multiple of the chip interval, and we compare the results with the symbol-synchronous case treated in [7]. Subsequently, we treat the more general asynchronous case; we show that the system can be represented as a chip-synchronous system with uniform timing jitter between zero and the chip interval for each interfering *user*. Note that this case differs from the situation treated in [1], in which each *pulse* suffers from an *independent* jitter.

The remainder of the paper is organized as follows. Section II describes the transmitted signal model and components of the received signal at the output of a matched filter (MF)

[1]This research is supported in part by the National Science Foundation under grant CCR-99-79361, and in part by the New Jersey Center for Wireless Telecommunications.

[2]Also at the Department of Electroscience, Lund University, Lund, Sweden.

[3]Since IR is a carrierless system, the only admissible phases are 0 and π. Therefore, BPSK becomes identical to Binary Amplitude-Shift Keying (BASK) in this case.

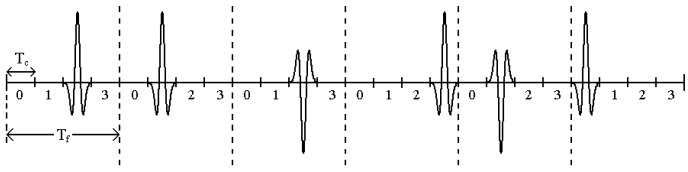

Fig. 1. A TH-IR signal with pulse-based polarity randomization where $N_f = 6$, $N_c = 4$ and the TH sequence is $\{2, 1, 2, 3, 1, 0\}$. Assuming that $+1$ is currently being transmitted, the polarity codes for the pulses are $\{+1, +1, -1, +1, -1, +1\}$.

receiver. The performance of chip-synchronous systems is analyzed in Section III. Section IV extends the results to asynchronous systems. After simulation studies in Section V, some concluding remarks are made in Section VI.

II. Signal Model

We consider a BPSK random time-hopping impulse-radio (TH-IR) system where the transmitted signal from user k in an N_u-user setting is represented by the following model:

$$s_{tx}^{(k)}(t) = \sqrt{\frac{E_k}{N_f}} \sum_{j=-\infty}^{\infty} d_j^{(k)}\, b_{\lfloor j/N_f \rfloor}^{(k)} w_{tx}(t - jT_f - c_j^{(k)} T_c), \quad (1)$$

where $w_{tx}(t)$ is the transmitted UWB pulse, E_k is the bit energy of user k, T_f is the average pulse repetition time (also called the "frame" time), N_f is the number of pulses representing one information symbol, and $b_{\lfloor j/N_f \rfloor}^{(k)} \in \{+1, -1\}$ is the information symbol transmitted by user k. In order to allow the channel to be exploited by many users and avoid catastrophic collisions, a time-hopping (TH) sequence $\{c_j^{(k)}\}$ is assigned to each user, where $c_j^{(k)} \in \{0, 1, ..., N_c - 1\}$ with equal probability, and $c_j^{(k)}$ and $c_i^{(l)}$ are independent for $(k, j) \neq (l, i)$. This TH sequence provides an additional time shift of $c_j^{(k)} T_c$ seconds to the jth pulse of the kth user where T_c is the chip interval and is chosen to satisfy $T_c \leq T_f / N_c$ in order to prevent the pulses from overlapping. Without loss of generality, $T_f = N_c T_c$ is assumed throughout the paper.

Random polarity codes $d_j^{(k)}$ are binary random variables taking values ± 1 with equal probability and $d_j^{(k)}$ and $d_i^{(l)}$ are independent for $(k, j) \neq (l, i)$ [7]. The receiver for user k is assumed to have the knowledge of polarity codes for that user.

An example signal is shown in Figure 1, where six pulses are transmitted for each information symbol ($N_f = 6$) with the TH sequence $\{2, 1, 2, 3, 1, 0\}$.

Using the signal model in (1), the received signal over an AWGN channel in an N_u-user system can be expressed as

$$\begin{aligned} r(t) &= \sum_{k=1}^{N_u} \sqrt{\frac{E_k}{N_f}} \sum_{j=-\infty}^{\infty} d_j^{(k)}\, b_{\lfloor j/N_f \rfloor}^{(k)} \\ &\times w_{rx}(t - jT_f - c_j^{(k)} T_c - \tau_k) + \sigma_n n(t), \end{aligned} \quad (2)$$

where τ_k is the delay of user k, $w_{rx}(t)$ is the received UWB pulse with unit energy and $n(t)$ is a zero mean white Gaussian noise process with unit spectral density. Although this channel model is not very realistic for UWB systems, it is an important first step towards understanding of more realistic channels, and also approximates the line-of-sight scenarios that are especially important for UWB systems. Furthermore, the main ideas of our analysis can be extended to multipath scenarios, though this is not elaborated here due to space limitations (see [9] for extensions to multipath channels).

We consider a matched filter (MF) receiver, where the template signal at the receiver can be expressed as follows:

$$s_{temp}^{(1)}(t) = \sum_{j=iN_f}^{(i+1)N_f - 1} d_j^{(1)} w_{rx}(t - jT_f - c_j^{(1)} T_c - \tau_1), \quad (3)$$

where, without loss of generality, user 1 is assumed to be the user of interest.

From (2) and (3), the MF output for user 1 can be expressed as follows:

$$y_1 = \sqrt{E_1 N_f}\, b_i^{(1)} + a + n, \quad (4)$$

where the first term is the signal part of the output, a is the multiple access interference (MAI) due to other users and n is the output noise, which can be shown to be distributed as $n \sim \mathcal{N}(0,\, N_f \sigma_n^2)$.

The MAI term can be expressed as the sum of interference terms from all $(N_u - 1)$ interfering users, that is, $a = \sum_{k=2}^{N_u} a^{(k)}$, where each interference term is in turn the summation of interference to one pulse of the template signal:

$$a^{(k)} = \sqrt{\frac{E_k}{N_f}} \sum_{l=iN_f}^{(i+1)N_f - 1} a_l^{(k)}, \quad (5)$$

where

$$\begin{aligned} a_l^{(k)} &= d_l^{(1)} \int w_{rx}(t - lT_f - c_l^{(1)} T_c - \tau_1) \sum_{j=-\infty}^{\infty} d_j^{(k)} \\ &\times b_{\lfloor j/N_f \rfloor}^{(k)} w_{rx}(t - jT_f - c_j^{(k)} T_c - \tau_k)\, dt. \end{aligned} \quad (6)$$

As can be seen from (6), $a_l^{(k)}$ denotes the interference from user k to the lth pulse of the template signal.

III. Chip-Synchronous Case

Assuming, without loss of generality, that $\tau_1 = 0$, τ_k is an integer multiple of T_c, for $k = 2, ..., N_u$, in the chip-synchronous case. More specifically, for user k, $\tau_k = \Delta_2^{(k)} T_c$, where $\Delta_2^{(k)} = 0, 1, ..., N - 1$ with equal probability, where $N = N_c N_f$ is the total number of chips per symbol. Let $\Delta_1^{(k)}$ be the offset between frames of user 1 and k. Then, $\Delta_1^{(k)} = \mod \{\Delta_2^{(k)}, N_c\}$ and obviously, $\Delta_1^{(k)} = 0, 1, ..., N_c - 1$ with equal probability (Figure 2). Also define $i_1^{(k)}$ as the number of frames of the template signal that overlap only with the $(i-1)$th symbol ($b_{i-1}^{(k)}$) of the signal from user k. That is,

$$i_1^{(k)} = \left\lfloor \frac{\Delta_2^{(k)}}{N_c} \right\rfloor, \quad (7)$$

with $\lfloor x \rfloor$ denoting the largest integer smaller than or equal to x.

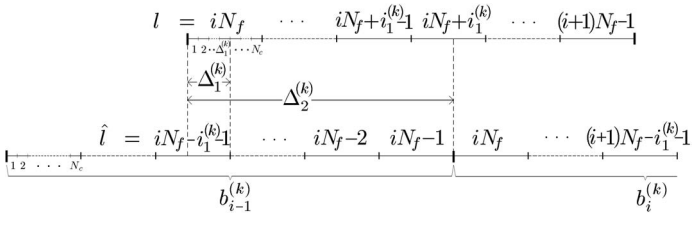

Fig. 2. The frame positions of the template signal (on the top) and the received signal from user k (on the bottom). Pulses are not shown.

Let $p_l^{(1)}$ denote the position of the lth pulse of the template signal in the lth frame ($p_l^{(1)} = 1, ..., N_c$) for $l = iN_f, ..., (i+1)N_f - 1$. Similarly, write $p_l^{(k)}$ for the position of the lth pulse of the received signal from user k. Then, depending on $p_l^{(1)}$, $a_l^{(k)}$ can be expressed as follows:

$$a_l^{(k)} = \begin{cases} \hat{b}_1 d_l^{(1)} d_{i-1}^{(k)} I_{\{p_l^{(1)}+N_c-\Delta_1^{(k)}=p_{i-1}^{(k)}\}} & \text{for } p_l^{(1)} = 1, ..., \Delta_1^{(k)} \\ \hat{b}_2 d_l^{(1)} d_i^{(k)} I_{\{p_l^{(1)}=p_i^{(k)}+\Delta_1^{(k)}\}} & \text{for } p_l^{(1)} = \Delta_1^{(k)}+1, ..., N_c \end{cases} \tag{8}$$

for $l = iN_f, ..., (i+1)N_f - 1$, where $\hat{l} = l - i_1^{(k)}$ and I_A is an indicator function taking value 1 in set A and 0 outside. Also

$$\hat{b}_1 = \begin{cases} b_{i-1}^{(k)}, & l = iN_f, ..., iN_f + i_1^{(k)} \\ b_i^{(k)}, & l = iN_f + i_1^{(k)} + 1, ..., (i+1)N_f - 1 \end{cases} \tag{9}$$

and

$$\hat{b}_2 = \begin{cases} b_{i-1}^{(k)}, & l = iN_f, ..., iN_f + i_1^{(k)} - 1 \\ b_i^{(k)}, & l = iN_f + i_1^{(k)}, ..., (i+1)N_f - 1. \end{cases} \tag{10}$$

In obtaining (8), the following observation is employed: When the lth pulse of the template signal is in one of the first $\Delta_1^{(k)}$ chips ($p_l^{(1)} = 1, ..., \Delta_1^{(k)}$), there can be interference from the $(l - i_1^{(k)} - 1)$th, that is, $(\hat{l} - 1)$th, pulse of user k if the pulses are in the same chip position, as indicated by the indicator function in the first line of (8). Also note that this interference to the lth pulse of the template signal is from the symbol $b_{i-1}^{(k)}$ when $l = iN_f, ..., iN_f + i_1^{(k)}$ and from the symbol $b_i^{(k)}$ when $iN_f + i_1^{(k)} + 1, ..., (i+1)N_f - 1$, as can be seen from Figure 2. Similar observations can be made when $p_l = \Delta_1^{(k)} + 1, ..., N_c$.

From the previous expressions, Lemma 3.1 follows when the number of pulses per information symbol is large:

Lemma 3.1: As $N_f \longrightarrow \infty$, the MAI from user k, $a^{(k)}$, is asymptotically normally distributed as

$$a^{(k)} \sim \mathcal{N}\left(0\,,\, \frac{E_k}{N_c}\right). \tag{11}$$

Proof: Considering $a_l^{(k)}$ given by (8), it is observed that $a_{iN_f}^{(k)}, ..., a_{(i+1)N_f-1}^{(k)}$ are identically distributed but are not independent. However, they form a 1-dependent sequence[4] since $a_{l_1}^{(k)}$ and $a_{l_2}^{(k)}$ are independent when $|l_1 - l_2| > 1$. Noting from (8) that $\mathrm{E}\{a_l^{(k)}\} = 0$ due to random polarity codes, the sum $\sqrt{\frac{E_k}{N_f}} \sum_{l=iN_f}^{(i+1)N_f-1} a_l^{(k)}$ converges to

$$\mathcal{N}\left(0\,,\, E_k[\mathrm{E}\{(a_{iN_f}^{(k)})^2\} + 2\mathrm{E}\{a_{iN_f}^{(k)} a_{iN_f+1}^{(k)}\}]\right). \tag{12}$$

for large N_f [11].

From (8), it can be shown that $\mathrm{E}\{(a_l^{(k)})^2\} = 1/N_c$ for all values of $\Delta_1^{(k)}$ using the fact that probability that a pulse is in a given chip is $1/N_c$. Furthermore, it can be observed that the correlation terms are zero due to random polarity codes. Therefore, $a^{(k)}$ given by (5) is asymptotically distributed as $\mathcal{N}(0\,,\, E_k/N_c)$. □

Note that this Gaussian approximation is different from the common normality assumption in the case of many users. Lemma 3.1 states that when the number of *pulses* per information symbol is large, MAI from an interfering user is approximately distributed as a Gaussian random variable. This is mainly due to the random polarity codes assigned to pulses of the user.

Also note that the asymptotic distribution of MAI for the chip-synchronous case is the same as that for the symbol synchronous case in [7]. In other words, for TH-IR systems with pulse-based polarity randomization, chip synchronism and symbol synchronism are equivalent in terms of the effects of MAI. The reason behind this is that probability that a pulse of the template signal and any pulse from an interfering user overlaps does not change whether the users are symbol-synchronized or chip-synchronized. The only difference in the chip-synchronous case is that this overlap to the lth pulse of the template can be caused by $(\hat{l}-1)$th pulse of the interfering user with probability $\Delta_1^{(k)}/N_c^2$ or by $\hat{l}$th pulse of that user with probability $(N_c - \Delta_1^{(k)})/N_c^2$.

From Lemma 3.1 and (4), bit error probability (BEP) can be expressed as follows for large N_f:

$$P_e \approx Q\left(\sqrt{\frac{E_1}{\frac{1}{N}\sum_{k=2}^{N_u} E_k + \sigma_n^2}}\right), \tag{13}$$

where $N = N_c N_f$, which can be defined as the total processing gain of the system. From this expression, it is observed that, systems with large total processing gain has lower probability of error since the probability of overlaps between the pulses of interfering users and those of the template signal decreases as N gets larger. Also it can be noted from (13) that probability of error depends on N_c and N_f only through their multiplication. Hence, the system performance does not change by changing the number of symbols per information symbol N_f and the number of chips per frame N_c as long as $N_c N_f$ is constant.

IV. Asynchronous Case

Now consider a complete asynchronous scenario where chip-synchronism is not assumed. Again assume $\tau_1 = 0$ without loss of generality. In this case, it is assumed that

[4] A sequence $\{X_n\}_{n\in\mathbb{Z}}$ is called a 1-dependent sequence, if any finite dimensional marginals $(X_{n_1}, ..., X_{n_i})$ and $(X_{m_1}, ..., X_{m_j})$ are independent whenever $m_1 - n_i > 1$.

$\tau_k \sim \mathcal{U}[0, NT_c)$ for $k = 2, ..., N_u$, where $\mathcal{U}$ denotes a uniform distribution.

In order to calculate the statistics of the MAI term in (4), the following simple result will be used.

Proposition 4.1: The MAI in the asynchronous case has the same distribution as the MAI in the chip-synchronous case with interfering user k having a jitter ϵ_k, for $k = 2, ..., N_u$, which is the same for all pulses of that user and is drawn from a uniform distribution given by $\mathcal{U}[0, T_c)$.

Proof: Consider (6). With $\tau_1 = 0$ without loss of generality, $\tau_k \in \{0, T_c, ..., (N-1)T_c\}$ with probability $1/N$ each in the chip-synchronous case. In the asynchronous case, $\tau_k \sim \mathcal{U}[0, NT_c)$, which has the same distribution as the sum of τ_k in the chip-synchronous case and a jitter ϵ_k with $\epsilon_k \sim \mathcal{U}[0, T_c)$. □

Proposition 4.1 reduces the problem to the calculation of the distribution of

$$a_l^{(k)} = d_l^{(1)} \int w_{rx}(t - lT_f - c_l^{(1)}T_c) \sum_{j=-\infty}^{\infty} d_j^{(k)} b_{\lfloor j/N_f \rfloor}^{(k)} \times w_{rx}(t - jT_f - c_j^{(k)}T_c - \tau_k - \epsilon_k)\, dt, \quad (14)$$

where $\tau_k \in \{0, T_c, ..., (N-1)T_c\}$ with equal probability and $\epsilon_k \sim \mathcal{U}[0, T_c)$. This problem is a special case of the analysis of TH-IR systems in the presence of timing jitter, which is studied in [1], with only difference being the fact that timing jitter is the same for all pulses of a user in this case instead of being independent identically distributed (i.i.d.) at each pulse.

The following lemma approximates the distribution of MAI from an asynchronous user, conditioned on the timing jitter of that user when the number of pulses per symbol, N_f, is large.

Lemma 4.1: As $N_f \longrightarrow \infty$, the MAI from user k, $a^{(k)}$, conditioned on the timing jitter ϵ_k is asymptotically normally distributed as

$$a^{(k)}|\epsilon_k \sim \mathcal{N}\left(0\,,\, \frac{E_k}{N_c}[R^2(\epsilon_k) + R^2(T_c - \epsilon_k)]\right), \quad (15)$$

where $R(x) = \int_{-\infty}^{\infty} w_{rx}(t) w_{rx}(t-x) dt$ is the autocorrelation function of the UWB pulse.

Proof: See Appendix A.

From Lemma 4.1, it is straightforward to show that the BEP of the system conditioned on the timing jitters of interfering users is given by

$$P_e|\boldsymbol{\epsilon} \approx Q\left(\frac{\sqrt{E_1}}{\sqrt{\frac{1}{N}\sum_{k=2}^{N_u}[R^2(\epsilon_k) + R^2(T_c - \epsilon_k)]E_k + \sigma_n^2}}\right), \quad (16)$$

where $N = N_c N_f$ and $\boldsymbol{\epsilon} = [\epsilon_2 \dots \epsilon_{N_u}]$.

Since $\epsilon_k \sim \mathcal{U}[0, T_c)$ for $k = 2, ..., N_u$, expectation of (16) with respect to $\boldsymbol{\epsilon}$ can be taken in order to obtain the BEP:

$$P_e \approx \frac{1}{T_c^{N_u - 1}} \int_0^{T_c} \dots \int_0^{T_c} P_e|\boldsymbol{\epsilon}\; d\epsilon_2 \dots d\epsilon_{N_u}. \quad (17)$$

However, when the number of users is large, calculation of (17) becomes cumbersome since it requires an integration over $(N_u - 1)$ variables. In this case, the following lemma can be employed to approximate the expression for BEP in the case of equal energy interferers.

Lemma 4.2: Assume that all interfering users have the same bit energy E. Then, as $N_u \longrightarrow \infty$, $a/\sqrt{N_u - 1}$, where a is the MAI term in (4), is asymptotically normally distributed as

$$\frac{a}{\sqrt{N_u - 1}} \sim \mathcal{N}\left(0\,,\, \frac{2E}{N_c T_c} \int_0^{T_c} R^2(\epsilon) d\epsilon\right). \quad (18)$$

Proof: See Appendix B.

Let $\gamma = \frac{2}{T_c}\int_0^{T_c} R^2(\epsilon) d\epsilon = \frac{1}{T_c}\int_{-T_c}^{T_c} R^2(\epsilon) d\epsilon$. Then, from (18), $a \sim \mathcal{N}(0\,,\, \gamma(N_u - 1)E/N_c)$. Note from (11) that for equal energy users, MAI in the chip-synchronous case is distributed as $a \sim \mathcal{N}(0\,,\, (N_u - 1)E/N_c)$. Hence it is observed that the difference between the powers of MAI terms depends on the autocorrelation function of the UWB pulse. For example, for the autocorrelation function in (21), $\gamma \approx 0.2$ and chip-synchronization assumption could result in over-estimating the error probability depending on the signal-to-interference-pulse-noise (SIR) ratio of the system.

From Lemma 4.2 and (4), the approximate expression for BEP is obtained as follows:

$$P_e \approx Q\left(\frac{\sqrt{E_1}}{\sqrt{(N_u - 1)\frac{2E}{NT_c}\int_0^{T_c} R^2(\epsilon) d\epsilon + \sigma_n^2}}\right), \quad (19)$$

for large values of N_u.

V. Simulation Results

In this section, BEP performance of a TH-IR system with pulse-based polarity randomization is evaluated by conducting simulations for different SIR values and for different number of interfering users. The following unit energy UWB pulses and autocorrelation functions are employed as the received UWB pulse, $w_{rx}(t)$, in the simulations (Figure 3):

$$w_1(t) = \left(1 - \frac{4\pi t^2}{\tau^2}\right) e^{-2\pi t^2/\tau^2} / \sqrt{E_p}\,, \quad (20)$$

$$R_1(\Delta t) = \left[1 - 4\pi(\frac{\Delta t}{\tau})^2 + \frac{4\pi^2}{3}(\frac{\Delta t}{\tau})^4\right] e^{-\pi(\frac{\Delta t}{\tau})^2}, \quad (21)$$

$$w_2(t) = \frac{1}{\sqrt{T_c}}, \quad -0.5T_c \le t \le 0.5T_c\,, \quad (22)$$

$$R_2(\Delta t) = \begin{cases} -\Delta t/T_c + 1, & 0 \le \Delta t \le T_c \\ \Delta t/T_c + 1, & -T_c \le \Delta t < 0 \end{cases}, \quad (23)$$

where E_p normalizes the energy of $w_1(t)$ to unity, $\tau = T_c/2.5$ is used in the simulations, and the rectangular pulse $w_2(t)$ is chosen as an approximate pulse shape in order to compare the performance of the system with different pulse shapes.

Figure 4 shows the BEP performance of a 10-user system ($N_u = 10$) where $N_f = 15$ and $N_c = 5$. The bit energy of the user of interest, user 1, is $E_1 = 0.5$, whereas the interfering users transmit bits with unit energy ($E_k = E = 1$ for $k = 2, ..., 10$), and the attenuation due to the channel is set equal to unity. The SIR is defined by the following equation

$$\text{SIR} = 10\log_{10}\left(\frac{E_1}{\frac{1}{N}\sum_{k=2}^{N_u} E_k + \sigma_n^2}\right). \quad (24)$$

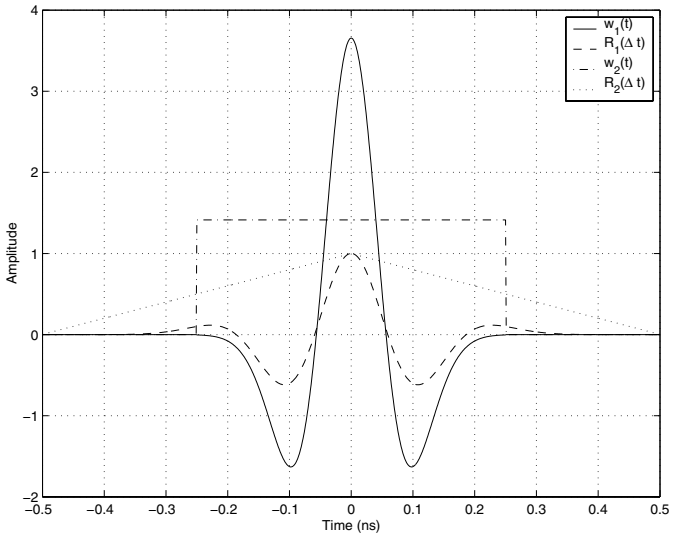

Fig. 3. UWB pulses and autocorrelation functions for $T_c = 0.5$ns.

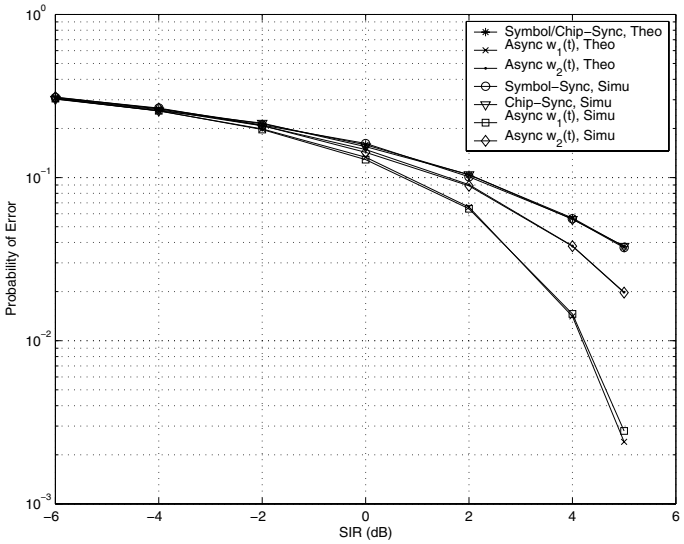

Fig. 4. BEP vs SIR for different cases, where $N_c = 5$, $N_f = 15$, $N_u = 10$, $E_1 = 0.5$ and $E = 1$.

In Figure 4, the SIR is varied by changing the noise power σ_n^2 and BEP is obtained for different SIR values in the cases of symbol-synchronous, chip-synchronous and asynchronous systems. For the asynchronous case, performance is simulated for different pulse shapes $w_1(t)$ and $w_2(t)$, given by (20) and (22), respectively. It is observed from the figure that the simulation results match closely with the theoretical results. Also note that for small SIR values, all the systems perform quite similarly since the main source of error is the thermal noise in that case. As the SIR increases, i.e., as MAI becomes more effective, the systems start to perform differently. The asynchronous systems perform better than the chip-synchronous and symbol-synchronous cases since $\frac{2}{T_c}\int_0^{T_c} R^2(\epsilon)d\epsilon$ in (19) is about 0.2 for $w_1(t)$ and $2/3$ for $w_2(t)$, which also explains the reason for the lowest BEP of the asynchronous system with UWB pulse $w_1(t)$. Also it is observed that chip-synchronous and symbol-synchronous systems perform the same as expected.

Figure 5 plots the BEP for different number of users for an asynchronous system employing the UWB pulse $w_1(t)$. Again $N_f = 15$ and $N_c = 5$ are used. In order to see the effects of MAI, the noise is set to zero, that is, $\sigma_n^2 = 0$. User 1 is again the user of interest with bit energy $E_1 = 0.5$ and interfering users are assumed to have the same bit energy of $E = 15$. It is observed from Figure 5 that as the number of user increases, the approximate BEP expression in (19) gets very close to the true probability of error. Also note that very accurate results are obtained if (17) is used. These results are shown for $N_u = 2, 3, 4$ only, since it becomes cumbersome to calculate them for a large number of users due to the requirement of integration over multiple variables.

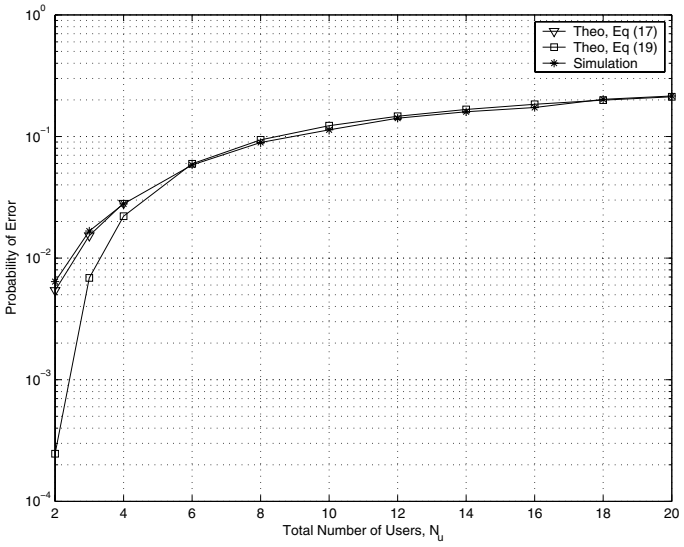

Fig. 5. BEP vs total number of users for an asynchronous system with $w_{rx}(t) = w_1(t)$, $N_c = 5$, $N_f = 15$, $E_1 = 0.5$ and $E = 15$ and $\sigma_n^2 = 0$.

VI. Conclusion

In this paper, the performance of TH-IR systems with pulse-based polarity randomization has been analyzed. First, a chip-synchronous system was considered and the approximate distribution of the MAI was derived, which was used to obtain a closed form BEP expression. It was observed that the chip-synchronous case has the same performance as the symbol synchronous case due to the presence of random polarity codes. Then, asynchronous systems were modelled as a chip synchronous system with uniform timing jitter for each interfering user, which lead to the extension of the results for the chip-synchronous case to the asynchronous systems. Also a closed-form expression was derived for the case of a large number of equal-energy users. Simulation results matched closely with the analytical expressions.

REFERENCES

[1] S. Gezici, H. Kobayashi, H. V. Poor, and A. F. Molisch, "The trade-off between processing gains of an impulse radio system in the presence of timing jitter," to be presented at the *IEEE International Conference on Communications (ICC 2004)*, Paris, France, June 2004.

[2] FCC 02-48: First Report and Order.

[3] M. Z. Win and R. A. Scholtz, "Impluse radio: How it works," *IEEE Communications Letters,* 2(2): pp. 36-38, Feb. 1998.

[4] M. Z. Win and R. A. Scholtz, "Ultra-wide bandwidth time-hopping spread-spectrum impulse radio for wireless multiple-access communications," *IEEE Transactions on Communications*, vol. 48, pp. 679-691, April 2000.

[5] D. Cassioli, M. Z. Win and A. F. Molisch, "The ultra-wide bandwidth indoor channel: from statistical model to simulations," *IEEE Journal on Selected Areas in Communications*, vol. 20, pp. 1247-1257, August 2002.

[6] C. J. Le-Martret and G. B. Giannakis, "All-digital PAM impulse radio for multiple-access through frequency-selective multipath," *IEEE Proc. Global Telecommunications Conference (GLOBECOM2000),* vol. 1, pp. 77-81, San Fransisco, CA, Nov. 2000.

[7] E. Fishler and H. V. Poor, "On the tradeoff between two types of processing gain," *40th Annual Allerton Conference on Communication, Control, and Computing,* Monticello, IL, Oct. 2-4, 2002.

[8] B. Sadler and A. Swami, "On the performance of UWB and DS-spread spectrum communications systems," *IEEE Proc. Conference of Ultra Wideband Systems and Technologies (UWBST'02),* pp. 289-292, Baltimore, MD, May 2002.

[9] S. Gezici, H. Kobayashi, H. V. Poor, and A. F. Molisch, "Performance Evaluation of Impulse Radio UWB Systems with Pulse-Based Polarity Randomization in Asynchronous Multiuser Environments," submitted to *IEEE Transactions on Signal Processing*, Nov. 2003.

[10] Y.-P. Nakache and A. F. Molisch, "Spectral shape of UWB signals influence of modulation format, multiple access scheme and pulse shape," *IEEE Proc. Vehicular Technology Conference, (VTC 2003-Spring)*, vol. 4, pp. 2510-2514, Jeju, Korea, April 2003.

[11] P. Billingsly, "*Probability and Measure,*" John Wiley & Sons, New York, 2nd edition, 1986.

APPENDIX

A. Proof of Lemma 4.1

In order to calculate the distribution of MAI $a=\sum_{k=2}^{N_u} a^{(k)}$, we first consider the MAI from one user, which is expressed as $a^{(k)}=\sqrt{\frac{E_k}{N_f}}\sum_{l=iN_f}^{(i+1)N_f-1} a_l^{(k)}$. The interference from user k to the lth pulse of the template signal, $a_l^{(k)}$, is given by (14), which can be expressed as follows, depending on the positions of the pulses:

Considering Figure 2, when the lth pulse of the template signal is in one of the first $\Delta_1^{(k)}$ chips, that is, for $p_l^{(1)}=1,...,\Delta_1^{(k)}$:

$$\begin{aligned} a_l^{(k)} &= \hat{b}_1 d_l^{(1)} d_{\hat{l}-1}^{(k)} [R(\epsilon_k) I_{\{p_l^{(1)}+N_c-\Delta_1^{(k)}=p_{\hat{l}-1}^{(k)}\}} \\ &\quad + R(T_c-\epsilon_k) I_{\{p_l^{(1)}+N_c-\Delta_1^{(k)}=p_{\hat{l}-1}^{(k)}+1\}}], \end{aligned} \tag{25}$$

for $l=iN_f,...,(i+1)N_f-1$, where $\hat{l}=l-i_1^{(k)}$ and $\hat{b}_1$ is as in (9). This equation is obtained by using the fact that in order for user k to interfere with the lth pulse of the template signal, a pulse from user k and the lth pulse of the template must be in the same chip positions, or user k's pulse must be in the previous chip and interfere with the lth pulse due to the timing jitter.

For $p_l^{(1)}=\Delta_1^{(k)}+1$, the interference to the lth pulse of the template signal can be expressed as follows:

$$\begin{aligned} a_l^{(k)} &= \hat{b}_2 d_l^{(1)} d_{\hat{l}}^{(k)} R(\epsilon_k) I_{\{p_{\hat{l}}^{(k)}=1\}} \\ &\quad + \hat{b}_1 d_l^{(1)} d_{\hat{l}-1}^{(k)} R(T_c-\epsilon_k) I_{\{p_{\hat{l}-1}^{(k)}=N_c\}}, \end{aligned} \tag{26}$$

for $l=iN_f,...,(i+1)N_f-1$, where $\hat{b}_2$ is as in (10).

Finally, for $p_l^{(1)}=\Delta_1^{(k)}+2,...,N_c$:

$$\begin{aligned} a_l^{(k)} &= \hat{b}_2 d_l^{(1)} d_{\hat{l}}^{(k)} [R(\epsilon_k) I_{\{p_{\hat{l}}^{(1)}=p_{\hat{l}}^{(k)}+\Delta_1^{(k)}\}} \\ &\quad + R(T_c-\epsilon_k) I_{\{p_l^{(1)}=p_{\hat{l}}^{(k)}+\Delta_1^{(k)}+1\}}], \end{aligned} \tag{27}$$

for $l=iN_f,...,(i+1)N_f-1$.

Similar to the proof of Lemma 3.1, $a_{iN_f}^{(k)},...,a_{(i+1)N_f-1}^{(k)}$ form a 1-dependent sequence. It can be shown that $\mathrm{E}\{a_l^{(k)}|\epsilon_k\}=0$, $\mathrm{E}\{(a_l^{(k)})^2|\epsilon_k\}=\frac{1}{N_c}[R^2(\epsilon_k)+R^2(T_c-\epsilon_k)]$ and $\mathrm{E}\{a_l^{(k)}a_{l+1}^{(k)}|\epsilon_k\}=0$. Hence $a^{(k)}$ conditioned on ϵ_k is distributed as follows for large N_f:

$$a^{(k)}|\epsilon_k \sim \mathcal{N}\left(0\,,\,\frac{E_k}{N_c}[R^2(\epsilon_k)+R^2(T_c-\epsilon_k)]\right). \tag{28}$$

B. Proof of Lemma 4.2

When the interfering users have equal bit energy E, the MAI $a=\sum_{k=2}^{N_u} a^{(k)}$ is the sum of (N_u-1) i.i.d. random variables with $a^{(k)}=\sqrt{\frac{E}{N_f}}\sum_{l=iN_f}^{(i+1)N_f-1} a_l^{(k)}$ for $k=2,\ldots,N_u$.

From the proof in Appendix A, we have $\mathrm{E}\{a_l^{(k)}|\epsilon_k\}=0$, $\mathrm{E}\{(a_l^{(k)})^2|\epsilon_k\}=\frac{1}{N_c}[R^2(\epsilon_k)+R^2(T_c-\epsilon_k)]$ and $\mathrm{E}\{a_l^{(k)}a_{l+1}^{(k)}|\epsilon_k\}=0$. Hence we obtain $\mathrm{E}\{a^{(k)}\}=0$ and $\mathrm{Var}\{a^{(k)}\}=\frac{E}{N_c}\mathrm{E}\{R^2(\epsilon_k)+R^2(T_c-\epsilon_k)\}$. As $N_u\longrightarrow\infty$, $a/\sqrt{N_u-1}$ converges to the following distribution by the Central Limit Theorem (CLT):

$$\frac{a}{\sqrt{N_u-1}} \sim \mathcal{N}\left(0\,,\,\frac{E}{N_c}[\mathrm{E}\{R^2(\epsilon)\}+\mathrm{E}\{R^2(T_c-\epsilon)\}]\right), \tag{29}$$

since $\epsilon_2,...,\epsilon_{N_u}$ are i.i.d. Also note that the subscript k is dropped from the jitter index in (29).

Using the fact that $\epsilon\sim\mathcal{U}[0,T_c)$, $\mathrm{E}\{R^2(\epsilon)\}+\mathrm{E}\{R^2(T_c-\epsilon)\}$ can be expressed as

$$\frac{1}{T_c}\int_0^{T_c}[R^2(\epsilon)+R^2(T_c-\epsilon)]d\epsilon=\frac{2}{T_c}\int_0^{T_c}R^2(\epsilon)d\epsilon. \tag{30}$$

Then, from (29) and (30), (18) follows.